International Journal of Automotive and Mechanical Engineering (IJAME)
ISSN: 2229-8649 (Print); ISSN: 2180-1606 (Online); Volume 11, pp. 2294-2305, January-June 2015

DOI: http://dx.doi.org/10.15282/ijame.11.2015.12.0193

NANOFLUIDS HEAT TRANSFER ENHANCEMENT THROUGH STRAIGHT CHANNEL UNDER TURBULENT FLOW

M. Kh. Abdolbaqi[1*], C.S.N. Azwadi[3], R. Mamat[1], W.H. Azmi[1,2] and G. Najafi[4]

[1]Faculty of Mechanical Engineering, Universiti Malaysia Pahang,
26600 Pekan, Pahang, Malaysia
[*]Email: abdolbaqi.mk@gmail.com
Phone: +601121752996; Fax: +6094246222
[2]Automotive Engineering Centre, Universiti Malaysia Pahang,
26600 Pekan, Pahang, Malaysia
[3]Faculty of Mechanical Engineering, Universiti Teknologi Malaysia,
81200 Skudai, Johor Bahru, Malaysia
[4]Tarbiat Modares University, Tehran, Iran

ABSTRACT

The need for high thermal performance thermal systems has been eventuated by finding different ways to enhance heat transfer rates. This paper introduces and analyzes numerically the heat transfer enhancement of nanofluids with different volume concentrations under turbulent flow through a straight channel with a constant heat flux condition. Solid nanoparticles of TiO_2 and CuO were suspended in water as a base fluid to prepare the nanofluids. CFD analysis is conducted by FLUENT software using the finite volume method. The heat flux considered is 5000 W/m^2, the Reynolds numbers are 10^4–10^6 with a constant volume concentration of 1–3%. Based on the analysis of the numerical results, it is found that the heat transfer rates and wall shear stress increase with increase of the nanofluid volume concentration. It appears that the CuO nanofluid significantly enhances the heat transfer. Furthermore, the numerical results are validated with the literature data available and show good agreement, with 4% deviation. The study concluded that the enhancement of the friction factor and Nusselt number is by 2% and 21%, respectively for the nanofluids at all Reynolds numbers. Therefore, nanofluids are considered to have great potential for heat transfer enhancement and are applied in heat transfer processes.

Keywords: Nanofluid; heat transfer; straight channel; CFD.

INTRODUCTION

Using heat transfer enhancement techniques can improve the thermal performance of a channel. Heat transfer techniques can be classified into three broad techniques: passive techniques that do not need external power such as rough surfaces, swirl flow devices, treated surfaces, extended surfaces, displaced enhancement devices, surface tension devices, coiled tubes and additives such as nanoparticles; active techniques that need external power to enable the desired flow modification to increase the heat transfer such as electrostatic fields, mechanical aids, jet impingement, suction, injection, surface vibration, and fluid vibration; compound techniques that are a mix of two or more of the abovementioned techniques. There are many applications of heat transfer augmentation by using nanofluids to ensure the cooling challenge necessary [1-3], such as in

photonics, transportation, electronics, and energy supply industries. [4-10] examined the effect of volume fraction and temperature on the viscosity of water-based TiO_2, SiO_2 and Al_2O_3 nanofluids [11-13]. Results were recorded and analyzed within a temperature range of 25–70 ^oC and volume concentrations of 0.1, 0.4, 0.7 and 1%. The viscosity of the nanofluid was experimentally measured by Bobbo, Fedele [14] utilizing a rheometer. It was obtained as a function of the nanoparticles shear rate and mass fraction. A double tube coaxial heat exchanger heated by solar energy using aluminum oxide nanofluid was presented experimentally and numerically by Luciu, Mateecsu [15]. Their results showed that the heat transfer performance of nanofluid is higher than base fluid. Water was already used as a base fluid for two non-similar materials, titanium dioxide (TiO_2) and single wall carbon nanohorn (SWCNH). The results showed the empirical correlation equations of viscosity. The turbulent flow of CuO, Al_2O_3 and TiO_2 nanofluids with different volume concentrations flowing through a two-dimensional duct under constant heat flux condition has been analyzed numerically [16].

In this study, heat transfer enhancement in a straight channel is carried out. The CFD analysis is performed using FLUENT software with the finite volume method. The heat flux, Reynolds numbers and the volume concentration are 5000 W/m^2, 10^4–10^6, and 1–3% respectively. The nanofluids TiO_2 and CuO dispersed in water are utilized. The results are compared with experimental data available in the literature for validation.

NUMERICAL MODEL

The numerical calculation was carried out using CFD code (ANSYS FLUENT 15) for the studied geometries. The governing equations were solved at every cell for all values of flow, pressure and temperature. The first step involves the creation of the three-dimensional geometric models of the undertaken problem using a design modeler, and the second step is model mesh generation in ANSYS software. The straight channel geometry considered is illustrated in Figure 1. In the current study, to represent flow in the numerical simulation the Cartesian coordinate system (x, y, z) was used. The heat transfer and turbulent flow were established simultaneously downstream in the channel. Additionally, the inlet boundary conditions of the water or nanofluid were set as velocity inlets; likewise, the pressure outlets were selected for the outlet boundary conditions. Moreover, a constant heat flux of 5000 w/m^2 was applied to the exterior wall. The tube material is copper, the physical properties of which are taken as constant density q = 8978 kg/m^3, specific heat C_p = 381 J/(kg K), and thermal conductivity K = 387.6 W/(m K).

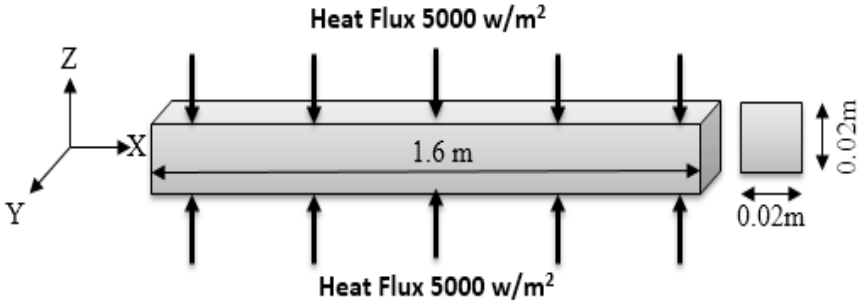

Figure 1. Cartesian geometry coordinates of problem undertaken.

Grid Independence Test

Grid independence was tested in ANSYS FLUENT 15 software for the channel with 40x40x160 cells and subdivisions in the axial length, and surface face, respectively. To find the most suitable size of mesh face, a grid independence test was performed for the physical model. In this study, rectangular cells were used to mesh the surfaces and wall of the channel. The grid independence was checked by using different grid systems, and three mesh faces were considered 20×20×160, 40×40×160 and 20×20×200 for pure water. The Nusselt numbers estimated for all four mesh faces and results were satisfactory. Throughout the iterative process, accurate monitoring of the residuals was done. When the residuals for all governing equations were lower than 10^{-6}, all solutions were assumed to be converged. Finally, the results could be obtained when the ANSYS FLUENT 15 iterations led to converged results defined by a set of converged criteria. The friction factor and Nusselt number inside the channel could be obtained throughout the computational domain in the post-process stage. This can be seen in Figure 2.

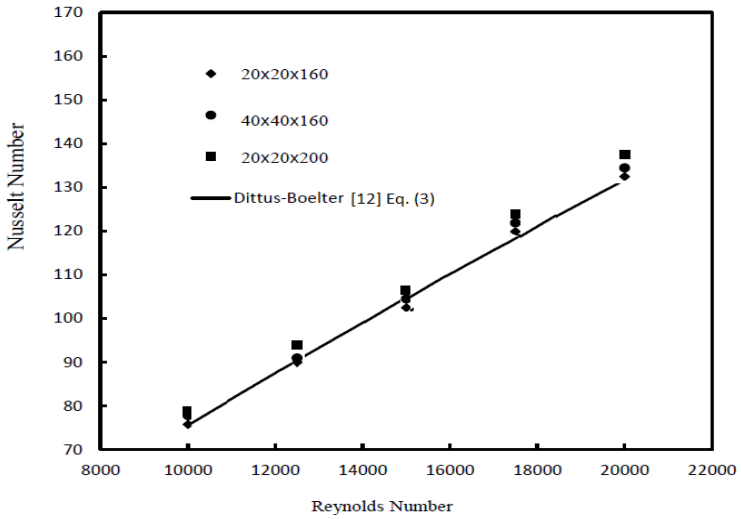

Figure 2. Grid independence test.

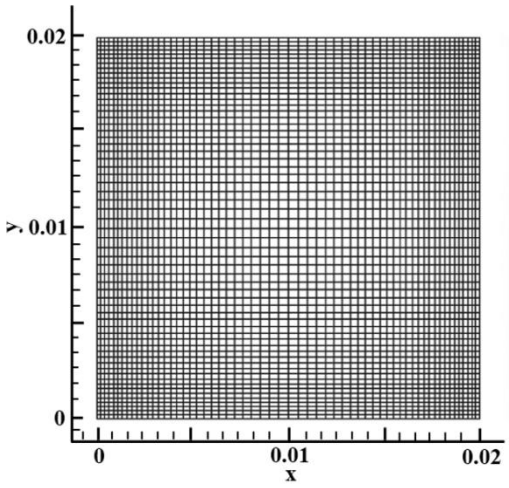

Figure 3. Model mesh.

The grid independence test of the Nusselt number against Reynolds number was performed with respect to all the grid mesh sizes. All of the meshing sizes appeared to be satisfactory, but in this study the mesh size 40x40x160 was be considered as the optimum meshing size. Although any number of mesh faces for these four cases can be used, the mesh faces with 40x40x160 were the best in terms of accuracy, as shown in Figure 3.

Physical Model

The assumptions made for this study are limited to steady state, incompressible and Newtonian turbulent fluid flow, constant thermo-physical properties of nanofluid, no effect of gravity, and heat conduction in the axial direction. High Reynolds numbers as input parameters were estimated; a pressure treatment with a 3D realizable k–□ turbulent model with enhanced wall treatment was employed, and converged solutions were considered for residuals lower than 25,000 for all the governing equations. The results of the simulation for the circular tube with nanofluids were compared with the equations of Blasius [17] in Eq. (1) for the friction factor and Dittus and Boelter [18] in Eq. [19] for the Nusselt number. The assumption of the problem undertaken is that the nanofluid behaves as a Newtonian fluid for concentrations less than 4.0% [20-22]. For conditions of dynamic similarity of the flow of the two media, nanoparticles and base fluid in the tube, the friction coefficients can be written as follows [17].

$$f_f = \frac{0.3164}{\mathrm{Re}^{0.25}} \tag{1}$$

The system of governing criteria can be written as follows:

A number of investigators derive the empirical correlation from experimental data [23-25].

$$f_r = \frac{f_{nf}}{f_f} = 1.078\left[\left(\frac{\rho_{nf}}{\rho_f}\right)^{-0.514}\left(\frac{\mu_{nf}}{\mu_f}\right)^{-0.1248}\right] \tag{2}$$

The forced convection heat transfer coefficient under turbulent flow may be estimated according to Dittus and Boelter [18] in Eq. (3) for the base fluid in the range of Reynolds number $10^4 < \mathrm{Re} < 10^5$.

$$Nu = \frac{h_f}{k_f} D = 0.023\,\mathrm{Re}^{0.8}\,\mathrm{Pr}^{0.4} \tag{3}$$

The modified Dittus–Boelter Eq. (4) is applicable for both base fluid and nanofluids with spherical-shaped nanoparticles dispersed in water as in (4).

$$Nu_{nf} = \frac{h_{nf}}{k_{nf}} D = 0.023\,\mathrm{Re}^{0.8}\,\mathrm{Pr}_f^{0.4}\left(1+\mathrm{Pr}_{nf}\right)^{-0.012}\left(1+\phi\right)^{0.23} \tag{4}$$

The Reynolds number depending on the diameter of the tube can be defined as:

$$\mathrm{Re} = \frac{\rho_{nf} \times D \times u}{\mu_{nf}} \tag{5}$$

GOVERNING EQUATIONS

The realizable *k*-□ turbulence model with wall heat treatment is used for turbulent flow simulation. The recent realizable turbulence model by Shih, Liou [27] is the most sophisticated model of the three k-ε differences and is characteristics by two main variations from the standard k–ε model. It utilizes a new equation for the turbulent viscosity equation and derives the dissipation rate transport equation from the mean-square vorticity fluctuation equation. Turbulent kinetic energy, k, and turbulent dissipation rate, ε, are combined with the governing equations using the relation of the turbulent viscosity $\mu_t=\rho C_\mu K^2/\varepsilon$, where $C_\mu=0.09$ and the following values have been assigned in the ANSYS FLUENT inputs as empirical constants:
$C_2=1.9$, $\sigma_\tau=0.85$, $\sigma_\kappa=1.0$, and $\sigma_\varepsilon=1.2$.

$$k = \frac{3}{2}(u.I)^2 , \varepsilon = C_\mu^{3/4} \frac{k^{3/2}}{L} \tag{6}$$

Furthermore, the character *L* in Eq. (6) refers to the turbulent characteristic length scale, which is set to be 0.07(d/2) in the current study. In addition, the factor of 0.07 has been adopted based on the maximum value of the mixing length in fully developed turbulent pipe flow. For an initial guess at the turbulent quantities (*k* and *ε*), the turbulent intensity (*I*) was specified, where the turbulent intensity for each case can be calculated based on Eq. (7) [28].

$$I = 0.16 \times \mathrm{Re}^{-1/8} \tag{7}$$

With regard to the nanofluid, infinitesimal (less than 100 nm) solid particles are assumed to be able to use a single phase approach, so the single phase approach is adopted for nanofluid modeling. For all these assumptions, the dimensional conservation equations for steady state mean conditions are as in the following continuity, momentum and energy equations Eqs. (8-10).

$$\frac{\partial u}{\partial x} + \frac{1}{r}\frac{\partial}{\partial r}(r\rho_{nf} u) = 0 \tag{8}$$

$$u\frac{\partial u}{\partial x} + v\frac{\partial}{\partial r}(\rho_{nf} u) = -\frac{\partial p}{\partial x} + \frac{1}{r}\frac{\partial}{\partial r}\left[r(\upsilon + \varepsilon_H)\frac{\partial u}{\partial r}\right] \tag{9}$$

$$\frac{1}{r}\frac{\partial}{\partial r}(\rho u T) = \frac{1}{r}\frac{\partial}{\partial r}\left[r(\alpha + \varepsilon_H)\frac{\partial T}{\partial r}\right] + \frac{1}{r^2}\frac{\partial}{\partial x}\left\{ \frac{k_{nf}}{C_p}\frac{\partial T}{\partial x}\right\} \tag{10}$$

The properties of solid particles are taken to be constant in the present operating conditions of 293 K to about 320 K. Therefore, in our simulations the properties of nanofluids are temperature-dependent. Table 1 shows the properties of nanofluids at the inlet section of the channel.

Table 1. Effective thermophysical properties of CuO–water and TiO_2–water ϕ in the range of 1–3 % and d_p=20 nm.

Thermo-physical property	d_p=20 nm CuO			TiO_2		
	ϕ=1%	ϕ=2%	ϕ=3%	ϕ=1%	ϕ=2%	ϕ=3%
$\rho\ (\frac{kg}{m^3})$	1050.8	1104	1157.1	1030.2	1062.8	1095.3
$C_p(\frac{J}{kg.K})$	3960	3762.1	3582.4	4034.79	3899.52	3772.3
k $(\frac{W}{m.K})$	0.616	0.632	0.65	0.615	0.63	0.6464
$\mu\ (\frac{Ns}{m^2})$	0.00103	0.00243	0.00267	0.00132	0.00154	0.0018

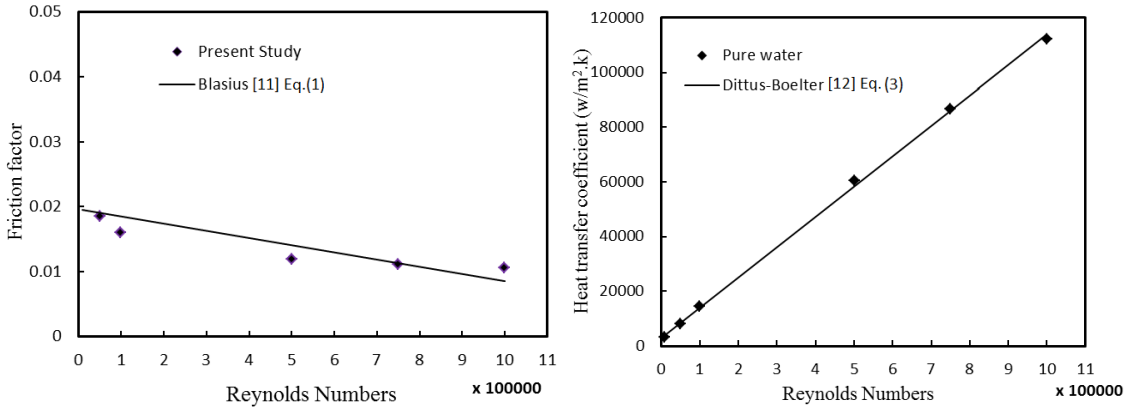

(a) Friction factor (b) Heat transfer coefficient

Figure 4. Verification process.

RESULTS AND DISCUSSION

Verification Process

The verification process is very important to check the results. It can be seen in Figure 4(a) that the friction factor decreases with increasing Reynolds number under the turbulent flow condition. The Blasius [17] Eq. (1) results are indicated as a solid black line. It appears that there is good agreement among the CFD results and the equation. On the other hand, the results of the heat transfer coefficient are shown in Figure 4(b). The Dittus and Boelter [18] Eq. [19] is indicated also, as a solid black line. It seems that there is good agreement between the CFD analysis and the equation. Figure 5 shows a comparison among the computed values of the Nusselt numbers and the equations given by Gnielinski [31-33] for TiO_2 nanofluid. As shown, an excellent agreement is observed with the computed values from the theoretical equation, over the range of Reynolds numbers studied. The Gnielinski [31] and Pak and Cho [33] correlations are indicated as a dotted black and solid black lines respectively.

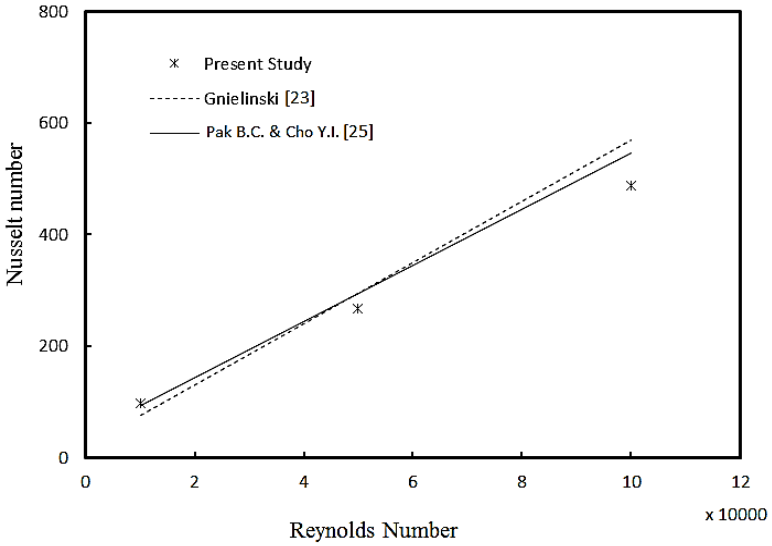

Figure 5. Nusselt numbers validation.

Effect of Nanofluid Type

Figure 6(a) shows the comparison of the friction factor CFD analysis results for pure water and TiO_2 and CuO nanofluids under the turbulent regime. There seems to be an insignificant effect of the type of nanofluid on the friction factor under turbulent flow conditions. Likewise, Figure 6(b) indicates the Nusselt number with Reynolds number for pure water and TiO_2 and CuO nanofluids under the turbulent regime. It can be seen that CuO nanofluid has the highest Nusselt number values, followed by TiO_2. The reason for CuO having the highest Nusselt number values may be that it also has the highest values of thermal conductivity and lowest viscosity.

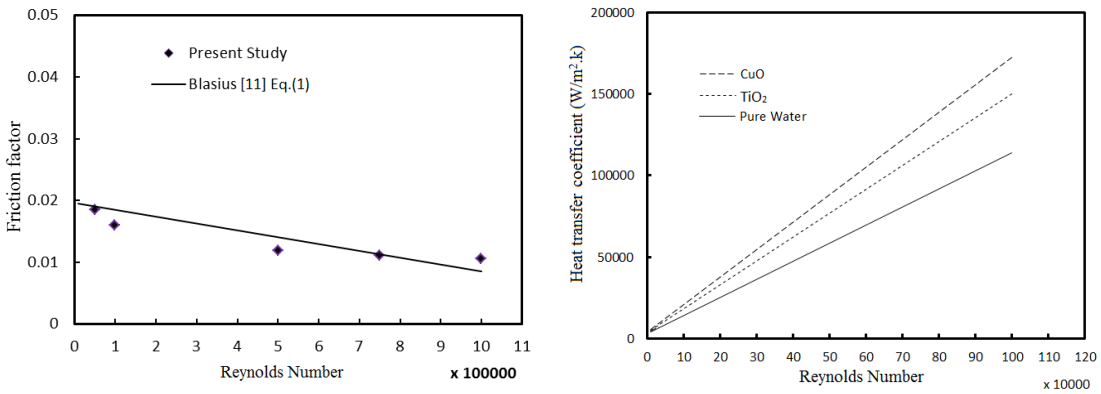

(a) Friction factor (b) Heat transfer coefficient

Figure 6. Effect of nanofluid type on the heat transfer coefficient at Reynolds numbers.

Figure 7 illustrates the local Nusselt numbers for CuO and TiO_2 nanofluid with volume fraction and nanoparticles diameter of 3% and 20 nm respectively. The result indicates that increasing the Reynolds number causes an increase in the local

Nusselt number. This is due to the fact that a higher Reynolds number leads to a higher velocity and temperature gradient at the channel [34].

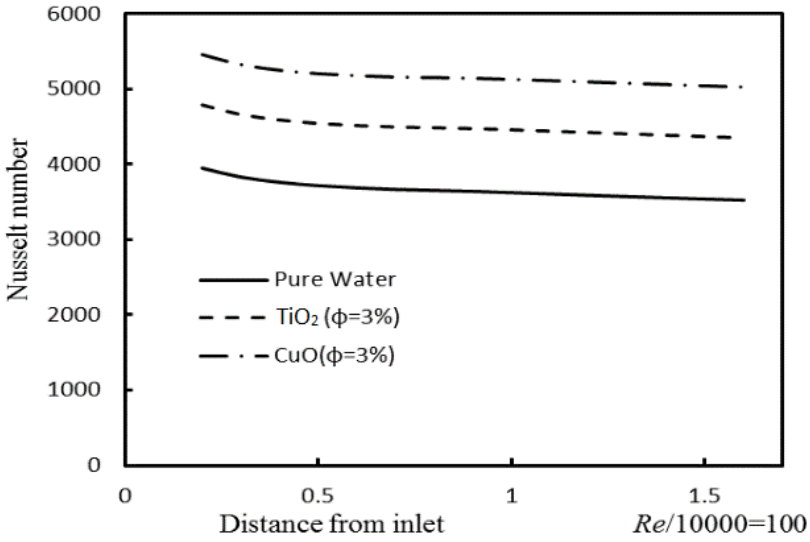

Figure 7. Local Nusselt number with length of channel.

Effect of Concentration on Heat Transfer Enhancement

The heat transfer coefficient with the Reynolds number for CuO nanofluid and 1–3% volume fraction is demonstrated in Figure 8. The effect of the nanofluid volume fraction appears to be significant. The heat transfer coefficient for pure water is also indicated, as a solid black line. The maximum enhancement is 10% when the volume fraction increased from 1 to 3%. The heat transfer coefficient appeared to be affected significantly by increase of the Reynolds number and nanofluid volume fraction [35]. The thermal conductivity of nanoparticles plays a significant role in the enhancement of nanofluids heat transfer [5].

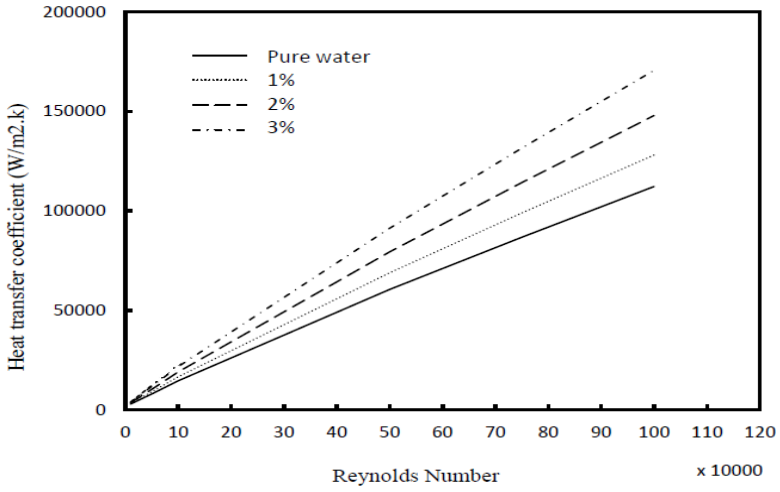

Figure 8. Effect of nanofluid concentration on the heat transfer coefficient at Reynolds numbers.

Effect of Nanoparticles Type and Concentration on Wall Shear Stress

The variation of the wall shear stress for CuO and TiO_2 nanofluids with respect to the distance from the inlet section of the channel at Reynolds number 10^6 and ϕ=3 is plotted in Figure 9. It can be observed that the wall shear stress varies depending on the type of nanoparticles. This condition is due to the variation in effective dynamic viscosity for different types of nanofluid [20].

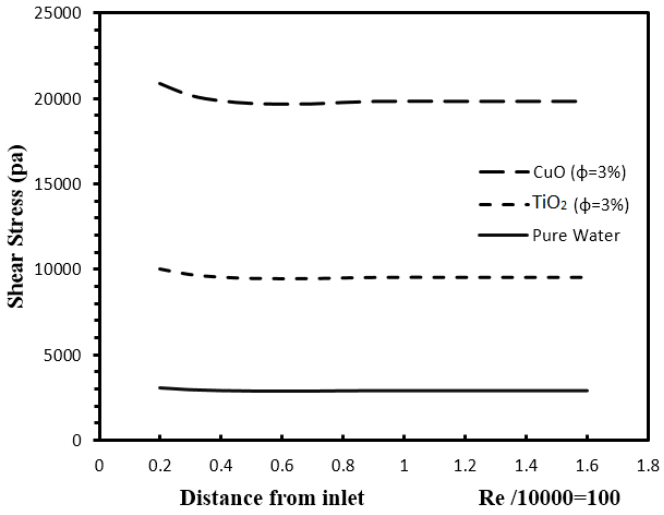

Figure 9. Shear stress for CuO and TiO_2 nanofluids with respect to inlet distance.

Figures 10 shows the relationship between the Reynolds number and the shear stress for different volume concentrations, ϕ=1, 2 and 3%. The shear stress increases with Reynolds number. Further, it will increase the secondary flow, decrease the thermal boundary layer and subsequently increase the Nusselt number [16, 36]. The reduction in velocities leads to increase in wall shear resistance and subsequently provides more heat dissipation with the nanofluids [35, 37].

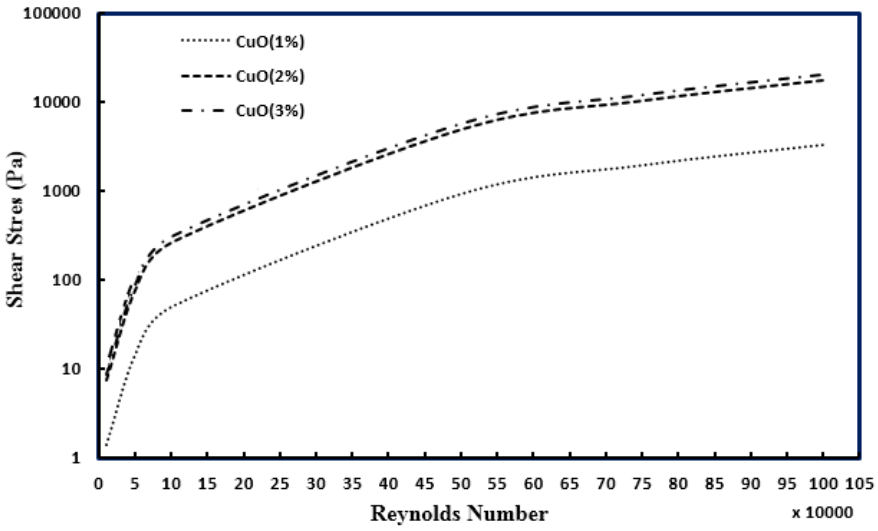

Figure 10. Reynolds number and shear stress for different volume fractions.

CONCLUSIONS

In the present study, the thermal properties of two types of nanoparticle suspended in water have been investigated numerically in forced convection heat transfer under turbulent flow with the uniform heat flux boundary condition of a straight channel. The heat transfer enhancement resulting from various parameters such as nanoparticle concentration of volume, and Reynolds number are reported. The finite volume method is used to solve the governing equations with certain assumptions and appropriate boundary conditions. The Nusselt number and friction factor are obtained through the numerical simulation. The study concluded that the enhancement of the friction factor and Nusselt number is by 2% and 21%, respectively for the nanofluids at all Reynolds numbers. The 3% volume concentration of nanofluid has the highest friction factor values, followed by 2% and 1%. The CFD analysis of pure water's friction factor at the channel has higher values than in a circular tube, as estimated using the Blasius equation. The Nusselt number of CuO has the highest value, followed by TiO_2. There is good agreement between the CFD analysis of the friction factor and the Nusselt number of the nanofluids with experimental data in the literature, with a deviation of not more than 4%.

ACKNOWLEDGEMENTS

The financial support by Universiti Malaysia Pahang (UMP) under RDU1403110 and also Automotive Excellence Center (AEC) under RDU1403153 are gratefully acknowledged.

REFERENCES

[1] Syam Sundar L, Sharma KV. An experimental study on heat transfer and friction factor of Al2O3 nanofluid. Journal of Mechanical Engineering and Sciences. 2011;1:99-112.

[2] Mahendran M, Lee GC, Sharma KV, Shahrani A. Performance of evacuated tube solar collector using water-based titanium oxide nanofluid. Journal of Mechanical Engineering and Sciences. 2012;3:301-10.

[3] Hussein AM, Sharma KV, Bakar RA, Kadirgama K. Heat transfer enhancement with nanofluids – A review. Journal of Mechanical Engineering and Sciences. 2013;4:452-61.

[4] Abdolbaqi MK, Azwadi CSN, Mamat R. Heat transfer augmentation in the straight channel by using nanofluids. Case Studies in Thermal Engineering. 2014;3:59-67.

[5] Azmi WH, Sharma KV, Mamat R, Anuar S. Nanofluid properties for forced convection heat transfer: an overview. Journal of Mechanical Engineering and Sciences. 2013;4:397-408.

[6] Azmi WH, Sharma KV, Sarma PK, Mamat R, Anuar S, Dharma Rao V. Experimental determination of turbulent forced convection heat transfer and friction factor with SiO_2 nanofluid. Experimental Thermal and Fluid Science. 2013;51:103-11.

[7] Azmi WH, Sharma KV, Sarma PK, Mamat R, Anuar S. Comparison of convective heat transfer coefficient and friction factor of TiO_2 nanofluid flow in

a tube with twisted tape inserts. International Journal of Thermal Sciences. 2014;81:84-93.

[8] Azmi WH, Sharma KV, Sarma PK, Mamat R, Najafi G. Heat transfer and friction factor of water based TiO_2 and SiO_2 nanofluids under turbulent flow in a tube. International Communications in Heat and Mass Transfer. 2014;59:30-8.

[9] Usri NA, Azmi WH, Mamat R, Abdul Hamid K. Viscosity of Aluminium Oxide (Al_2O_3) Nanoparticle Dispersed in Ethylene Glycol. Applied Mechanics and Materials. 2014;660:735-9.

[10] Zakaria I, Azmi WH, Mohamed WANW, Mamat R, Najafi G. Experimental Investigation of Thermal Conductivity and Electrical Conductivity of Al_2O_3 Nanofluid in Water-Ethylene Glycol Mixture for Proton Exchange Membrane Fuel Cell Application. International Communications in Heat and Mass Transfer. 2015;61:61-8.

[11] Hussein AM, Bakar RA, Kadirgama K, Sharma KV. Experimental measurements of nanofluids thermal properties. International Journal of Automotive and Mechanical Engineering. 2013;7:850-63.

[12] Mahendran M, Lee GC, Shahrani A, Bakar RA, Kadirgama K. Diurnal pattern and estimation of global solar radiation in East Coast Malaysia. International Journal of Automotive and Mechanical Engineering. 2013;8:1162-75.

[13] Ravisankar B, Tara Chand V. Influence of nanoparticle volume fraction, particle size and temperature on thermal conductivity and viscosity of nanofluids- A review. International Journal of Automotive and Mechanical Engineering. 2013;8:1316-38.

[14] Bobbo S, Fedele L, Benetti A, Colla L, Fabrizio M, Pagura C, et al. Viscosity of water based SWCNH and TiO_2 nanofluids. Experimental Thermal and Fluid Science. 2012;36:65-71.

[15] Luciu RS, Mateecsu T, Cotorobai V, Mare T. Nusselt Number and Convection Heat Transfer Coefficient for a Coaxial Heat Exchanger using Al_2O_3-Water pH ¼ 5 Nanofluid. Bul Inst Polit Iasi. 2009;55:71-80.

[16] Rostamani M, Hosseinizadeh SF, Gorji M, Khodadadi JM. Numerical study of turbulent forced convection flow of nanofluids in a long horizontal duct considering variable properties. International Communications in Heat and Mass Transfer. 2010;37:1426-31.

[17] Blasius H. Das Aehnlichkeitsgesetz bei Reibungsvorgängen in Flüssigkeiten. Mitteilungen über Forschungsarbeiten auf dem Gebiete des Ingenieurwesens. 1913;131.

[18] Dittus FW, Boelter LMK. Heat transfer in automobile radiators of the tubular type: University of California Publications on Engineering 2; 1930.

[19] Zhang H, Wu Q, Lin J, Chen J, 124304. ZXAP. Thermal conductivity of polyethylene glycol nanofluids containing carbon coated metal nanoparticles. J Appl Phys. 2010;108:124304–9.

[20] Azmi WH, Sharma KV, Mamat R, Alias ABS, Izwan Misnon I. Correlations for thermal conductivity and viscosity of water based nanofluids. IOP Conf Series: Materials Science and Engineering. 2012;36:1 - 6.

[21] Nguyen CT, Desgranges F, Roy G, Galanis N, Maré T, Boucher S, et al. Temperature and particle-size dependent viscosity data for water-based nanofluids - Hysteresis phenomenon. International Journal of Heat and Fluid Flow. 2007;28:1492-506.

[22] Gupta S, Sharma R, Soni SK, Sharma S. Biomass utilization of waste algal consortium for extraction of algal oil Journal of Algal Biomass Utilization. 2012;3:34-8.
[23] Duangthongsuk W, Wongwises S. Heat transfer enhancement and pressure drop characteristics of TiO_2-water nanofluid in a double-tube counter flow heat exchanger. International Journal of Heat and Mass Transfer. 2009;52:2059-67.
[24] Leong KY, Saidur R, Kazi SN, Mamun AH. Performance investigation of an automotive car radiator operated with nanofluid-based coolants (nanofluid as a coolant in a radiator). Applied Thermal Engineering. 2010;30:2685-92.
[25] Durmuş A, Durmuş A, Esen M. Investigation of heat transfer and pressure drop in a concentric heat exchanger with snail entrance. Applied Thermal Engineering. 2002;22:321-32.
[26] Duangthongsuk W, Wongwises S. An experimental study on the heat transfer performance and pressure drop of TiO2-water nanofluids flowing under a turbulent flow regime. International Journal of Heat and Mass Transfer. 2010;53:334-44.
[27] Shih T-H, Liou WW, Shabbir A, Yang Z, Zhu J. A new k-ϵ eddy viscosity model for high reynolds number turbulent flows. Computers and Fluids. 1995;24:227-38.
[28] Fluent A. Ansys Fluent Theory Guide. ANSYS Inc, USA. 2011.
[29] Bejan A. Porous and complex flow structures in modern technologies: Springer Science & Business Media; 2004.
[30] Manning R, Ewing, J. (2009). .RACQ Vehicles Technologies. Temperatures in cars survey. RACQ Vehicles Technologies. 2009:1-21.
[31] Gnielinski V. New equations for heat and mass transfer in turbulent pipe and channel flow. International Chemical Engineering. 1976;16:359-68.
[32] Bejan A, Kraus AD. Heat transfer handbook: John Wiley & Sons; 2003.
[33] Pak BC, Cho YI. Hydrodynamic and heat transfer study of dispersed fluids with submicron metallic oxide particles. Experimental Heat Transfer. 1998;11:151-70.
[34] Zhu Z, Yang H, Chen T. Numerical study of turbulent heat and fluid flow in a straight square duct at higher Reynolds numbers. International Journal of Heat and Mass Transfer. 2010;53:356-64.
[35] Azmi WH, Sharma KV, Sarma PK, Mamat R, Anuar S, Syam Sundar L. Numerical Validation of Experimental Heat Transfer Coefficient with SiO_2 Nanofluid Flowing in a Tube with Twisted Tape Inserts. Applied Thermal Engineering. 2014;73:294-304.
[36] Maïga SEB, Nguyen CT, Galanis N, Roy G. Heat transfer behaviours of nanofluids in a uniformly heated tube. Superlattices and Microstructures. 2004;35:543-57.
[37] Sarma PK, Subramanyam T, Kishore PS, Rao VD, Kakac S. A new method to predict convective heat transfer in a tube with twisted tape inserts for turbulent flow. International Journal of Thermal Sciences. 2002;41:955-60.